Coupling Zero-Valent Iron and Fenton processes for degrading sulfamethazine, sulfathiazole, and norfloxacin

iThe corrections made in this section will be reviewed and approved by a journal production editor.

Ana Luiza Fornazaria anafornazari@gmail.com fornazari@iqsc.usp.br Vanessa Feltrin Labriola a* vanlabri@hotmail.com vanlabri@usp.br Bianca Ferreira da Silva b biribisfs@gmail.com bianca.ferreira-silva@unesp.br Lucas Fernandes Castro c lcsfernandes75@gmail.com lucasfernandes@usp.br Janice Rodrigues Perussi c janice@iqsc.usp.br Eny Maria Vieira d eny@iqsc.usp.br Eduardo Bessa Azevedo a bessa@iqsc.usp.br

aUniversity of São Paulo (USP), São Carlos Institute of Chemistry, Laboratório de Desenvolvimento de Tecnologias Ambientais (LDTAmb), Avenida Trabalhador São-Carlense, 400 – Centro, São Carlos, SP, Brazil

bSão Paulo State University (UNESP), Araraquara Chemistry Institute, Departamento de Química Analítica, Rua Prof. Francisco Degni, 55 – Quitandinha, Araraquara, SP, Brazil

cUniversity of São Paulo (USP), São Carlos Institute of Chemistry, Grupo de Fotosensibilizadores, Avenida Trabalhador São-Carlense, 400 – Centro, São Carlos, SP, Brazil

dUniversity of São Paulo (USP), São Carlos Institute of Chemistry, Grupo de Química Analítica Ambiental e Ecotoxicologia, Avenida Trabalhador São-Carlense, 400 – Centro, São Carlos, SP, Brazil

*Corresponding author.

ABSTRACT Abstract

In this study, the degradation of three antibiotics — sulfamethazine (SMT), sulfathiazole (STZ), and norfloxacin (NOR) (1.0 mg L^{-1} each) — was achieved by coupling the Zero-Valent Iron Process using supported metallic iron nanoparticles (nZVI) to the Fenton one. The system was operated in single-pass continuous-flow mode at steady-state regime (after 15 min). The nanoparticles were packed into a fixed-bed reactor and characterized by several techniques (SEM, EDX, TEM, and XRD). The degradation experiments were performed according to a 2^2 factorial design, in which the effects of pH and flow rate (Q) were studied. The degradation conditions were: initial pH = 3.0 and Q = 20 mL min^{-1}. H_2O_2 was then continuously added to the effluent of the nZVI reactor (containing Fe^{2+}) in order to perform the Fenton process in the following mixing vessel (H_2O_2 concentration of 34 mg L^{-1}). At the exit of the system, the antibiotics concentrations were below the detection limit of the chromatographic method (40 µg L^{-1}) and dissolved iron was below 1.0 mg L^{-1}. Sixteen degradation products (DPs) of SMT, STZ, and NOR were detected and identified using HPLC-MS/MS. Their ecotoxicological endpoints (LC_{50}, EC_{50}, and ChV) for three trophic levels were estimated with the aid of the ECOSAR 2.0 software. No ecotoxicity was generated towards *Lactuca sativa* during treatment. The proposed system was able to partially remove the antimicrobial activity (*Escherichia coli*) of both sulfonamides (16%) and NOR (47%).

Keywords:

Antimicrobial activity, Antibiotics, AOP, Nanoparticles, ZVI

1 INTRODUCTION Introduction

As pharmaceuticals are widely used in human and veterinary medicine, they end up being contaminants of environmental concern (CECs) in water bodies [1]. CECs are defined as

synthetic or naturally-occurring chemicals whose disposal is not yet legislated and their effects on the environment and human health are still unknown [2].

Several classes of pharmaceuticals and their metabolites are detected in aquatic environments at low concentrations (ng L^{-1} to µg L^{-1}) [3]. Those are (pseudo) persistent substances, which can cause serious damage to the environment and humans [4], as well as drug resistance among bacteria [5].

Antibiotics are molecules that can inhibit the growth of microorganisms. They may be natural (produced by bacteria and fungi), semi-synthetic (derived from natural antibiotics), or synthetic (chemically prepared) substances [6]. In this work, three different antibiotics were studied: two sulfonamides – sulfamethazine and sulfathiazole (SMT and STZ, respectively) – and one fluoroquinolone (norfloxacin, NOR).

Sulfonamides were the first safe and effective synthesized antimicrobial drugs, in 1936 [7]. Since then, several antibiotics were synthesized. Advances include: increased antibacterial power, decreased toxicity, and the introduction of compounds with special properties, such as high or low solubility and prolonged therapeutic effect. Examples of the latter are fluoroquinolones [8]. Fluoroquinolones were first introduced in the late 1980s. Shortly after, a second-generation of quinolones emerged, which included ciprofloxacin, enoxacin, lomefloxacin, norfloxacin, and ofloxacin [9].

SMT, STZ, and NOR have become ubiquitous in surface waters and wastewaters [1]. Studies have shown that conventional treatment processes are relatively ineffective for removing those pharmaceuticals from water. Therefore, it is crucial that new technologies, capable of removing those contaminants from water matrices, be developed [10].

Several studies have identified those antibiotics in water bodies, such as rivers [11], shrimp ponds in mangrove areas [12], wastewater sewage [13], domestic wastewaters [14], and hospital wastewaters [15].

The use of zero valent iron (ZVI) for treating contaminated waters has some benefits, like low toxicity, low cost, besides being easy to obtain [16]. In anoxic aqueous medium, the oxidation of Fe^0 occurs in two steps: First, Fe^0 reacts with one molecule of water to form HFe^IOH (Eq. (1)). Second, HFe^IOH reacts with another molecule of water, generating $Fe^{II}(OH)_2$ (Eq. (2)) [17]. In oxic conditions, oxygen is the electron acceptor, forming hydroxyl ion (Eq. 3) or even hydrogen peroxide, if the medium is acidic ~~(Equation~~(Eq. (4) ~~4))~~) [18].

$$Fe^0 + H_2O \rightarrow HFe^IOH \quad (1)$$
$$HFe^IOH + H_2O \rightarrow Fe^{II}(OH)_2 + 2H_2 \quad (2)$$
$$Fe^0 + O_2 + 2H_2O \rightarrow 2\,Fe^{2+} + 4\,OH^- \quad (3)$$
$$Fe^0 + O_2 + 2H_3O^+ \rightarrow Fe^{2+} + H_2O_2 + 2H_2O \quad (4)$$

The generated ferrous ions can be oxidized to ferric ions (Fe^{3+}), which in turn may react with hydroxyl ion or water, forming iron hydroxides or oxyhydroxides [19]. Ferric hydroxide can be dehydrated and form oxides. All of the species generated can react with organic compounds and oxidize or reduce them, depending on the reaction medium [20].

When Fe^0 generates ferrous and/or ferric ions with the formation or the addition of hydrogen peroxide, the Fenton process takes place. It is one of the Advanced Oxidation Processes (AOP), which use strong oxidizing agents (O_3, H_2O_2), catalysts (Fe, TiO_2), and/or light, for the degradation of organic substances in waters and wastewaters. AOPs are a financially feasible alternative that can be combined to conventional treatments [21].

The Zero-Valent Iron Process (ZVI) has been used mainly for the reduction of organochlorine and nitroaromatic compounds [32]. The process of using metallic iron particles (Fe^0) has been studied since the ~~'70~~'70s, but only since the ~~'90~~'90s have the studies on the remediation of organic pollutants via iron oxide oxidation become expressive [22,23]. The use of metallic nanoparticles for treating waters and wastewaters is recent, such as for the removal of the antibiotics: amoxicillin [24], metronidazole [25], ciprofloxacin [26], and metoprolol [27]. It has been used for the removal of lindane [28], lead ions [29], arsenic and

selenium [30], and perchlorate [31] from water. It has been used also for the remediation of polluted soil and groundwater [32].

In this study, supported zero-valent iron nanoparticles (nZVI), according to Ponder, Darab, and Mallouk [33], were synthesized and characterized − transmission electron microscopy (TEM), scanning electron microscopy (SEM), and energy-dispersive X-ray spectroscopy (EDX) −. The degradation performance of the supported nZVI followed by the Fenton process for degrading SMT, STZ, and NOR was investigated with the aid of a ~~full~~ factorial design. Degradation products were determined by high-performance liquid chromatography (HPLC) coupled to mass spectrometry (HPLC-MS/MS).

To our best knowledge, this is the second study dealing with a continuous system in which the ZVI process is physically separated from the oxidative one [34]. On the other hand, it is the first time that ① supported nZVI followed by the Fenton process were used to degrade SMT, STZ, and NOR and ② the biological inactivation of the treated effluent was assessed by determining its ecotoxicity (*Lactuca sativa*) and antibacterial activity (*Escherichia coli*).

2

~~MATERIALS AND METHODS~~Materials and methods

Analytical standards − sulfamethazine ($C_{12}H_{14}N_4O_2S$, 99,8%), sulfathiazole ($C_9H_9N_3O_2S_2$, 99,6%) and norfloxacin ($C_{16}H_{18}FN_3O_3$, 99,5%) − were purchased from Sigma-Aldrich and used as received.

Analytical grade reagents − sulfuric acid (H_2SO_4, 96%), sodium hydroxide (NaOH, 97%), iron(II) sulfate heptahydrate ($FeSO_4 \cdot 7H_2O$, 99.5%), peroxide hydrogen (H_2O_2, 30% in weight), sodium borohydride ($NaBH_4$, 98%), ethanol (CH_3OH, 99.8%) − and acetonitrile (HPLC grade) were purchased from Merck®, Istanbul.

2.1

Iron ~~Nanoparticles Synthesis~~nanoparticles synthesis

Iron nanoparticles can be produced by different methods, exhibiting quite different properties. They are reactive species and their surface properties change rapidly with time, solution chemistry, and environmental conditions [16].

Iron nanoparticles were synthesized according to Ponder, Darab, and Mallouk [33], by the reduction of ferrous ions with borohydride (Eq. 5).2 $Fe^{2+} + BH_4 + 2H_2O \rightarrow Fe^0$ (s) $+ BO_2^- + 4H^+ + 2H_2$ (g)(5)

In a typical synthesis, performed under a gentle stream of nitrogen, ~~10~~10 g $FeSO_4 \cdot 7H_2O$ were dissolved in ~~70~~70 mL distilled water. That solution was mixed with ~~30~~30 mL of ethanol and the resulting pH adjusted to 6.8 with diluted NaOH. Then, ~~4.0~~4.0 g of sand (thoroughly washed with distilled water, H_2SO_4 ~~0.03~~0.03 mol L^{-1}, and distilled water again) was added. Sand particles acted as a support for the growth of the iron nanoparticles. Finally, ~~2.0 g~~2.0 g $NaBH_4$ were slowly added under continuous magnetic stirring. The reaction mixture was kept under stirring for ~~20~~20 min and vacumm-filtered through a ~~0.45 μm~~0.45 μm cellulose acetate membrane. The filtered supported nanoparticles were washed twice with ethanol, dried for ~~1~~1 min, and stored in a desiccator under vacuum.

2.2

Iron ~~Nanoparticles Characterization~~nanoparticles characterization

Microphotographs were taken to determine the iron nanoparticles morphology and size. Scanning Electron Microscopy (SEM) was performed in a Leica-Zeiss LEO 440 microscope coupled to an Oxford 7060 X-ray microanalyzer. Transmission Electron Microscopy (TEM) was performed in a FEI TECNAI ~~G²~~G² F20 HRTEM coupled to a dispersive X-rays emission spectroscopy, operated with ~~10−25~~10–25 kV voltage acceleration and 70,000–280,000 magnifications. The synthesized iron nanoparticles were first dispersed in isopropyl

alcohol. Then, one drop of the suspension was poured on a carbon-coated copper grid, dried at room temperature, and taken to the microscope.

The chemical composition (%) was determined by Energy-Dispersive X-ray Spectroscopy (EDS) in an EDX LINK ANALYTICAL (Isis System Series 300) spectroscope equipped with a SiLi Pentafet detector (ATW II), 133 eV to 5.9 keV resolution, and 10 mm^2 area, coupled to a Leica-Zeiss LEO 440 microscope (SEM). Operational parameters were: copper calibration standard, 20 kV electron beam, 25 mm focal length, 30% dead time, 2.82 A current, and 2.5 nA I probe.

To identify the compounds present on the nanoparticles surface, X-ray Diffraction (XRD) analyses were performed in a Siemens D5000 diffractometer (Cu Kα radiation, $\lambda = 1.54056$ Å, graphite monochromator). The scanning speed was $1°\ \text{min}^{-1}$ between $5° < 2\theta < 75°$. The obtained diffractograms were compared to standards from the International Center for Diffraction Data (ICDD), PCPDFWIN crystallographic cards collection, v. 2.01.

The performed nanoparticles characterization can be found in the Supplementary Material.

2.3

Antibiotics degradation

Initially, the degradation by the nZVI process was optimized with the aid of a 2^2 factorial design (performed in duplicate). The factors were pH and flow rate (Q). Alkaline solutions decrease degradation as iron(III) hydroxide tends to coat the iron nanoparticles surfaces, passivating them, as well as hindering the contact with potential pollutants [35]. On the other hand, as pH decreases, more iron leaching is observed. Therefore, pH levels were chosen to be 3.0 and 5.0.

Regarding Q, the levels were those representing the extreme operational conditions of the system (Fig. 1): 20 and $40\ \text{mL min}^{-1}$ (measured with a Dwyer Instruments Inc. #RMA-32-SSV rotameter). The storage tank and the vessels were made of borosilicate glass. They were connected by silicon and Tygon® tubings.

alt-text: Fig. 1

Fig. 1

- 0
-
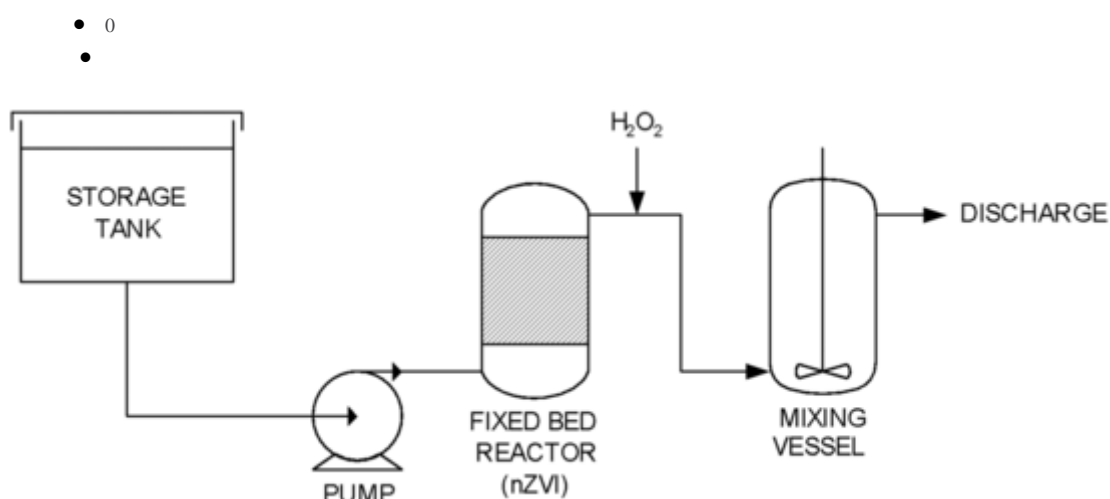
Simplified experimental setup scheme (not in scale).

The storage tank was fed with SMT, STZ, or NOR $(1.0\ \text{mg L}^{-1}$ each). The solution was then pumped through a fixed-bed reactor $(80\ \text{mL})$ packed with five layers (from the bottom): glass wool, 2 g sand, approximately 100 mg nZVI supported in 4.0 g sand, 2 g sand, and glass wool (Fig. 2). Between vessels, hydrogen peroxide $(170\ \text{mg L}^{-1})$ was continuously pumped (peristaltic pump IPC ISM931 #75M761A-0390) to achieve $34\ \text{mg H}_2\text{O}_2\ \text{L}^{-1}$ inside the mixing vessel.

Fig. 2

- 0
-

(a) (b)
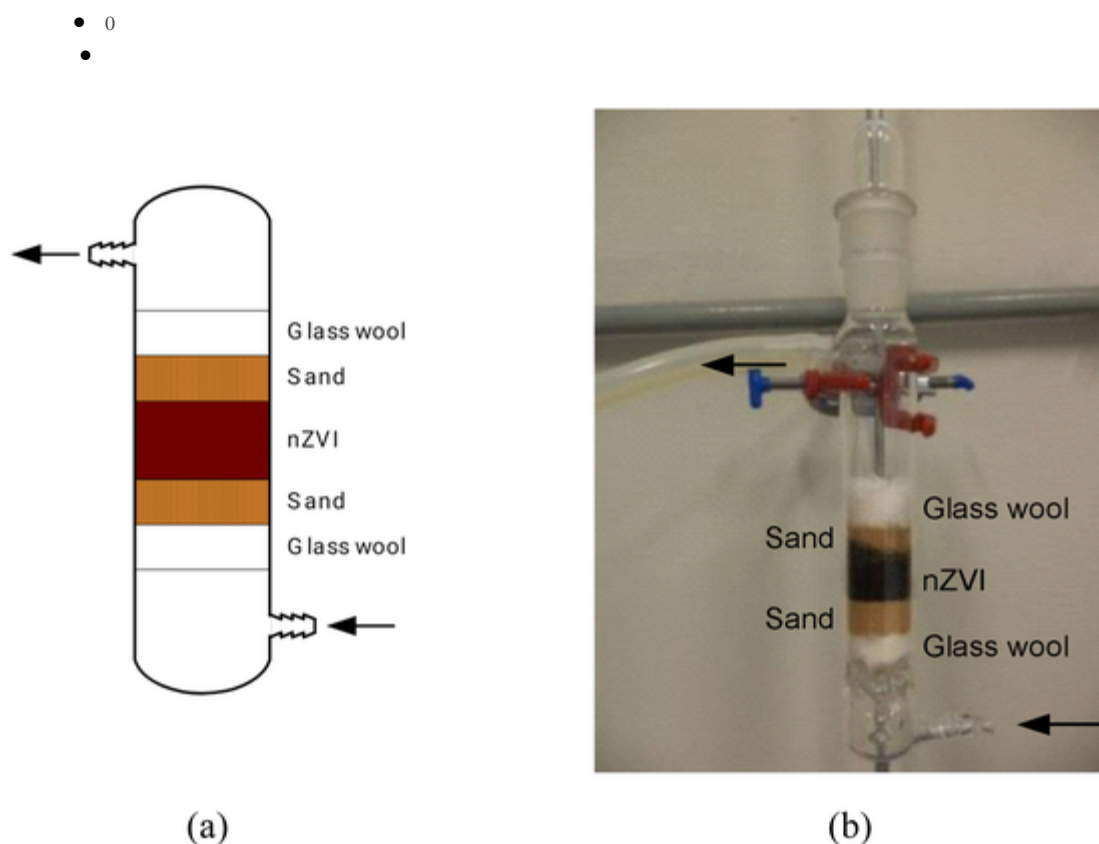
Fixed bed reactor: (a) drawing and (b) photograph.

All experiments were performed at room temperature. pH adjustments were made by diluted NaOH or H_2SO_4 solutions and pH values were measured with the aid of a Marconi PA200 ~~pHmeter.~~ pH meter. The system was operated in single-pass continuous flow mode. All analyses were performed at steady-state regime, which was achieved after ~~15~~15 min of operation.

2.4

Analyses

Residual iron was determined by the *o*-phenanthroline method 3500 [36]. A red complex called ferroin is formed with Fe^{2+}. The complex absorbance at 511 nm was recorded in a Varian Cary Win UV Scan Application spectrophotometer.

Residual hydrogen peroxide concentration was determined using the ammonium vanadate spectrophotometric method [37]. It is based on the red-orange peroxo-vanadium cation formation when H_2O_2 reacts with the metavanadate ion. That cation was monitored at ~~457~~457 nm, in the same spectrophotometer.

SMT, STZ, and NOR concentrations were measured by HPLC in an Agilent 1200 chromatograph with a 1260 DAD detector. Chromatographic conditions were: Agilent Zorbax ODS C18 ~~55 µm~~µm ~~(4.6 × 250~~ (4.6 × 250 mm) column at ~~30°C,~~30 °C, mobile phase 20:80% (in volume) mixture of ethanol:water, flow rate ~~0.4~~0.4 mL min^{-1}, injection volume ~~17~~17 µL, and detection wavelength ~~270~~270 nm. Run time was ~~6~~6 min plus ~~4~~4 min for cleaning the system.

Degradation products (DPs) of SMT and STZ were identified by HPLC-MS/MS coupling a mass spectrometer with a hybrid triple quadrupole/linear ion trap (3200 QTRAP, AB SCIEX) to the chromatograph. During those analyses, a C18 pre-column was used.

Operational parameters were: electrospray ionization (ESI) in negative mode, curtain gas pressure 15 psi, ion spray voltage 5200 V, gas 1 and 2 pressures 50 psi, temperature 450 °C, declustering potential 71/26 V, and entrance potential 10.00 V. Full scan range was from 100 to 400 Da. The mobile phase was the same used in the HPLC-DAD analyses. Injection volume was 10 µL and column temperature of 40ºC.

NOR concentrations and DPs were measured/identified by HPLC-MS/MS coupling a mass spectrometer with a hybrid triple quadrupole/linear ion trap (3200 QTRAP, AB SCIEX) to the chromatograph. The column was an Agilent Zorbax ODS C18 5 µm (4.6 × 250 mm) equipped with a C18 guard column, which was maintained at 40 °C. The mobile phase consisted of water acidified with 0.1% formic acid (A) and acetonitrile (B) with $Q = 1$ mL min^{-1}. The initial gradient conditions were 95% A for 10 min, decreased to 5% A over a period of 10–11 min and then increased to 95% A from 11 to 14 min; injection volume 10 µL, and detection wavelength 273 nm. Run time was 14 min plus 4 min for cleaning the system. Operational parameters of the mass spectrometer were: electrospray ionization (ESI) in positive mode, curtain gas pressure – 10 psi, ion spray voltage – 5500 V, gas 1 and 2 pressures – 50 psi, temperature – 700 °C, declustering potential – 46 V, and entrance potential – 5.00 V. Full scan range was from 100 to 400 Da. Injection volume was 10 µL and column temperature 40 ºC.

When studying the removal of pollutants, besides proving that the chosen degradation process is capable of significantly reducing the pollutant concentration, it is of utmost importance to check whether the pollutant ecotoxicity was also reduced/removed. Moreover, one should prove that no additional ecotoxicity was generated during the process [38]. Specifically, as the studied pollutants are antibiotics, the removal of their antimicrobial activity should be also evaluated, in order to predict whether resistant bacteria may be generated if the effluent of the process is discarded into a water body [39].

The ECOlogical Structure-Activity Relationship Model (ECOSAR) version 2.0 [40] was used to estimate the SMT, STZ, NOR, and their respective DPs ecotoxicological endpoints for three trophic levels: LC_{50} (fish and daphnid), EC_{50} (green algæ), and ChV (fish, daphnid, and green algæ).

Here, LC_{50} is a statistically-derived concentration in water of a substance that can be expected to cause death in 50% of the tested organisms (continuous exposure: fish − 96 h and daphnid − 48 h). EC_{50} is a statistically-derived concentration in water of a substance that can be expected to cause a specific effect (e.g., growth inhibition) in 50% of the tested organisms (96-h continuous exposure). ChV is the chronic value, i.e., the geometric mean between the no observed effect concentration − NOEC (highest tested concentration of a substance that produced no statistically significant effects) and the lowest observed effect concentration − LOEC (lowest concentration of a substance that produced statistically significant effects) [40].

Biological tests were performed in the initial solution, after the fixed-bed reactor, and after the mixing vessel. Acute ecotoxicity tests were performed, in quadruplicate, using *Lactuca sativa* seeds as the test-organism. Ten seeds were allowed to germinate on filter papers soaked with the test solution at several dilutions for 120 h (Petri dishes in the dark, 24 ± 1 °C). Afterwards, the hypocotyls (the stems of germinating seedlings, found below the cotyledons and above the radicles) were measured [41,42]. The more toxic the sample, the smaller the size of the hypocotyls.

Antibacterial activity tests with an *Escherichia coli* strain (ATCC 25922) were performed in a 96-wells plate to which 50 µL test solution, 50 µL Muller-Hinton broth, and 100 µL of a suspension containing 10^6 cells mL^{-1} (optical density 0.324 at 590 nm, Hitachi U-2800

spectrophotometer) were added. After incubating at 37ºC for 18 h with orbital shaking, samples were transferred to microtubes and centrifuged for 10 min at 1300 rpm. Supernatants were discarded and to the precipitate, 50 μL MTT (3-(4,5-dimethylthiazol-2-yl)− 2,5-diphenyltetrazolium bromide) at 2 mg mL^{-1} were added. Microtubes were incubated at 37ºC for 30 min and centrifuged for 5 min at 6000 rpm. Supernatants were once again discarded and to the precipitate, 150 μL isopropanol was added. The microtubes contents were vortex-mixed for 1 min. Finally, 50 μL phosphate-buffered saline (PBS) were added to the microtubes, which were vortex-mixed again (1 min) and the respective absorbances measured in a plate reader at 560 nm [43]. Tests were performed in triplicate.

3

RESULTS AND DISCUSSIONResults and discussion

3.1

Antibiotics Degradationdegradation

First, an aqueous solution of SMT and STZ (1.0(1.0 mg L^{-1} each) was fed to the fixed-bed reactor and the degradation experiments were performed according to the 2^2 factorial design. Then, in other experiments, NOR (1.0(1.0 mg L^{-1}) was also tested. The best results were achieved with the smallest tested Q and pH (Fig. 3).

alt-text: Fig. 3

Fig. 3

- 0
-

(a) (b) (c)
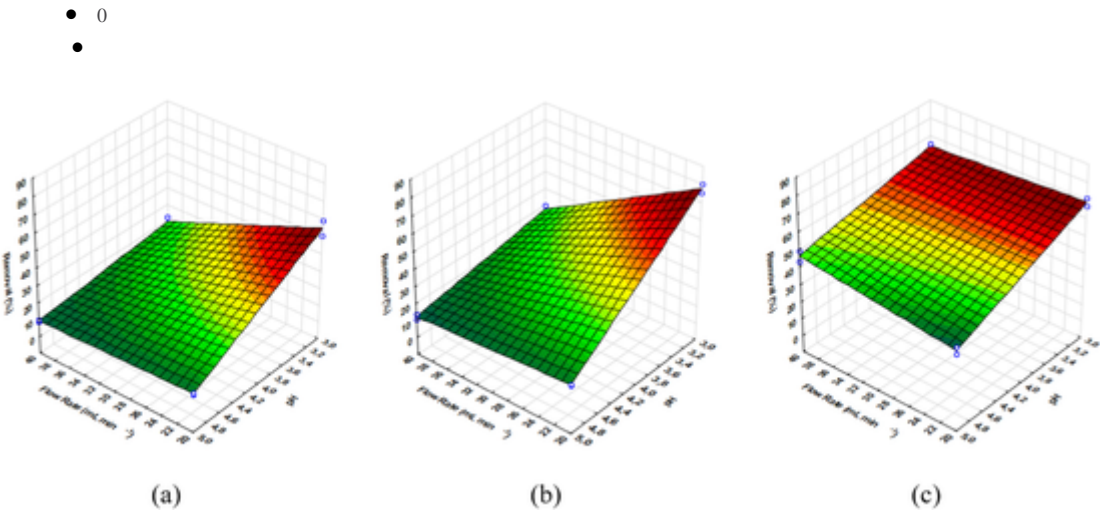
Response surfaces from the 2^2 factorial designs performed: (a) sulfamethazine, (b) sulfathiazole, and (c) norfloxacin.

The tendency of increasing degradation by decreasing Q and pH is clear. However, 2020 mL min^{-1} is the lowest attainable Q in the system used and a pH = 3.0= 3.0 is already far acidic; besides that, as acidity increases, so does iron leachability, which is by no means desirable. NOR degradation seems to be less sensitive to changes in the reactor operational conditions.

Therefore, Q = 20= 20 mL min^{-1} and pH = 3.0= 3.0 were set as the operational conditions. The system achieved the steady state after 1515 min for, at least, 66 h. The obtained results are summarized in Table 1. One can see that STZ was preferably degraded in comparison to SMT. This observation is in accordance with several works showing that SMT is more stable than STZ [44,45]. The smaller stability of STZ may be related to its amide-imide tautomerism. In average, the sulfonamides degradation was 66.3%, which is approximately the same degradation observed for NOR (68.9%). That finding may be an evidence of the nZVI process robustness.

alt-text: Table 1

Table 1

Performances of the nZVI process and of its coupling to the Fenton one. Antibiotics initial concentration: ~~1.0~~1.0 mg L^{-1}.

| Processes	Removal (%)			Residual
	SMT	STZ	NOR	(mg L^{-1})
1st)~~st~~ nZVI	54.8 ± 2.7	77.7 ± 1.9	68.9 ± 2.2	$6 - 9$
2nd)~~nd~~ Fenton**	> 96			< 1

*

~~**~~** All final concentrations were below the method detection limit.

The steady-state concentrations of total dissolved iron were ~~9.0~~9.0 mg L^{-1} (SMT and STZ) and ~~6.0~~6.0 mg L^{-1} (NOR). Taking advantage of this residual dissolved iron, hydrogen peroxide was continuously added after the fixed-bed reactor to perform the Fenton process, degrading the antibiotics even further. The target H_2O_2 concentration in the mixing vessel was always ~~34~~34 mg L^{-1}.

By coupling nZVI and Fenton processes, the steady-state concentrations of the antibiotics were all below the method detection limit (~~40~~(40 µg L^{-1}), which means a removal greater than 96%. Total dissolved iron concentration was also below the method detection limit (~~1.0~~(1.0 mg L^{-1}) (Fig. 4).

alt-text: Fig. 4

Fig. 4

- 0
-

(a)   (b)
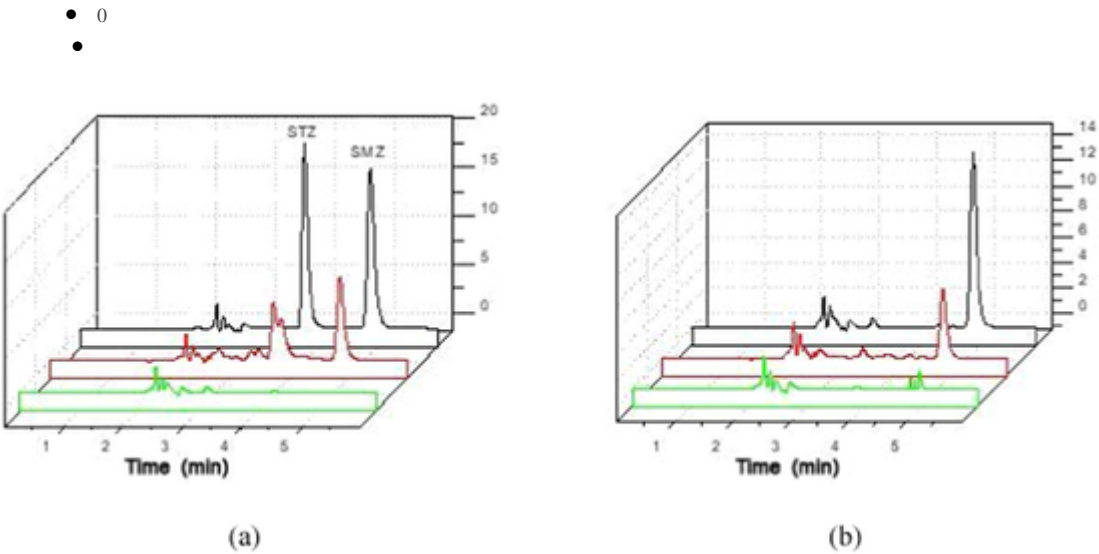
Chromatograms of removals using nZVI: (a) SMT and STZ ($\frac{1}{}$(1 mg L^{-1}); (b)

NOR ($\frac{1}{}$(1 mg L^{-1}). (━) initial solution of sulfonamides ($\frac{1}{}$(1 mg L^{-1} each); (   )

after nZVI; and (   ) after Fenton Process (pH 3 and flow rate of $\frac{20}{}$20 mL min^{-1}). It is worthwhile mentioning that the degradation kinetics was not studied because all results were obtained at steady-state conditions. Moreover, as the initial antibiotics concentrations were low ($\frac{1.0}{}$(1.0 mg L^{-1}), the carbon concentration of degraded samples were even lower, making it impossible to measure their organic carbon concentration and, therefore, the mineralization achieved.

3.2
Degradation ~~Products Identification~~products identification
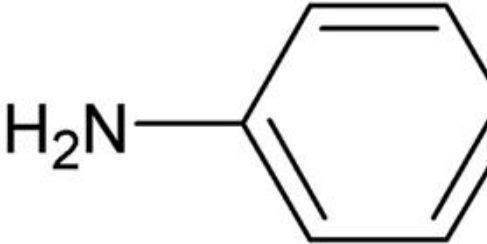
In the SMT degradation, three DP were identified (Table 2). Two different signals corresponded to the same mass and yielded the same mass spectra. Both isomers presented a base peak of m/z 215, corresponding to the elemental composition $C_{12}H_{15}N_4$ [46,47]. The DP with retention time (t_R) 1.70 min appears to be the product of a Smiles-type rearrangement followed by SO_2 extrusion [47,48] and the second one (t_R 4.31 min) was generated on account of the SO_2 removal [49]. SO_2 extrusion was often exhibited by sulfonamides in previous studies [47, 48, 50]. DP with m/z 295 ($C_{12}H_{14}N_4O_3S$) at 4.63 min can be assigned to hydroxylated sulfamethazine, generated when •OH attacks SMT at the α position (N − H bond on the benzene ring) [50]. The fragmentation mechanisms are given in the Supplementary Material.
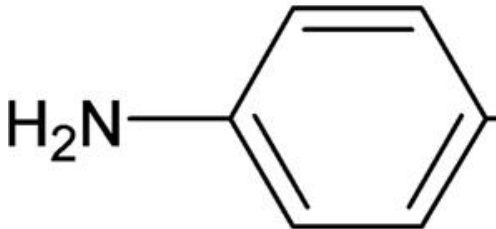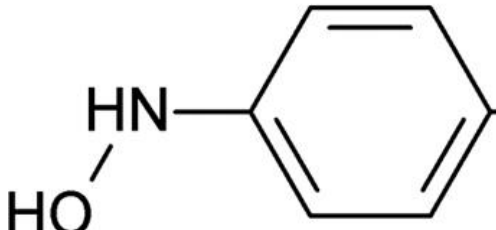
alt-text: Table 2

Table 2

iThe table layout displayed in this section is not how it will appear in the final version. The representation below is solely purposed for providing corrections to the table. To preview the actual presentation of the table, please view the Proof.

Main degradation products of sulfamethazine formed after coupling nZVI and Fenton processes, identified by HPLC-MS/MS, using the Lig

Degradation Products	Molecular formulas	m/z [M−H]$^+$	Proposed structures
1	$C_{12}H_{14}N_4$	215 → 198 → 156215 → 173	

Degradation Products	Molecular formulas	m/z [M−H]$^+$	Proposed structures
2	$C_{12}H_{14}N_4$	$215 \rightarrow 198 \rightarrow 188 \rightarrow 156$	
3	$C_{12}H_{14}N_4O_3S$	$295 \rightarrow 229295 \rightarrow 214295 \rightarrow 186 \rightarrow 122295 \rightarrow 107$	

During STZ degradation, five DP were identified (Table 3). As SMT, the first DP of STZ also shows SO_2 extrusion followed by SO_2 removal (m/z 192). DP with m/z 257 ($C_{12}H_{14}N_4O_3S$) is probably associated with the attack of •OH radicals to the benzene ring and can be assigned to hydroxyl-sulfathiazole [46,50]. The former may undergo cleavage, generating the DP with m/z 174 ($C_6H_7NO_3S$). DP with m/z 272 can be generated when •OH attacks STZ at the double bond position next to sulfur, giving the phenosulfazole ($C_9H_8N_2O_3S_2$). Also, STZ can form 2-aminothiazole ($C_3H_4N_2S$) with m/z 101 [51]. The fragmentation mechanisms are given in the Supplementary Material.
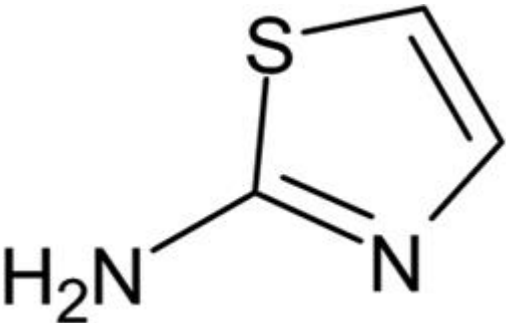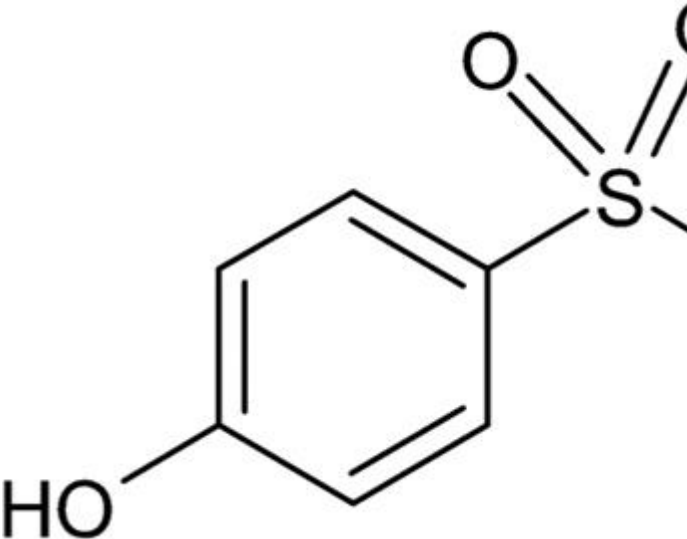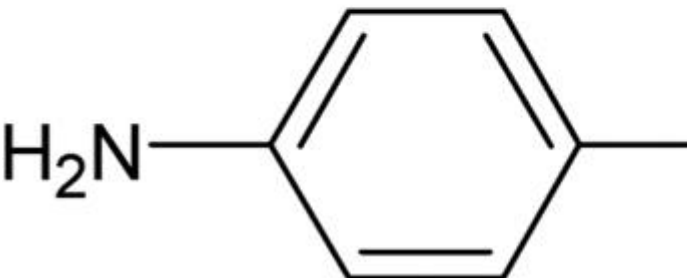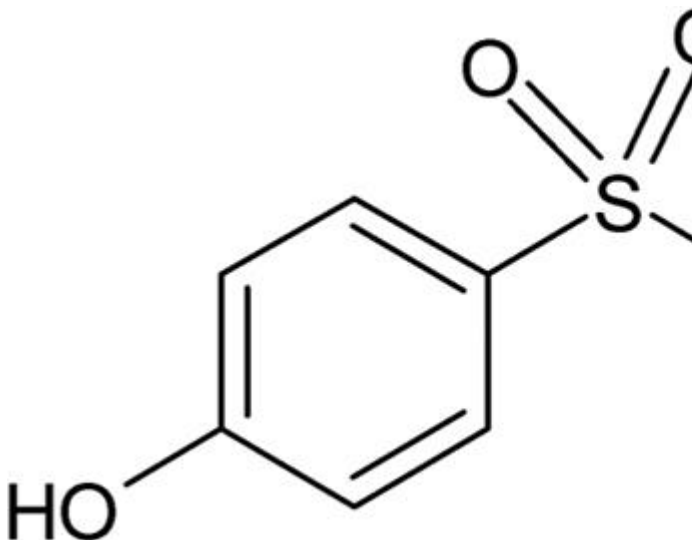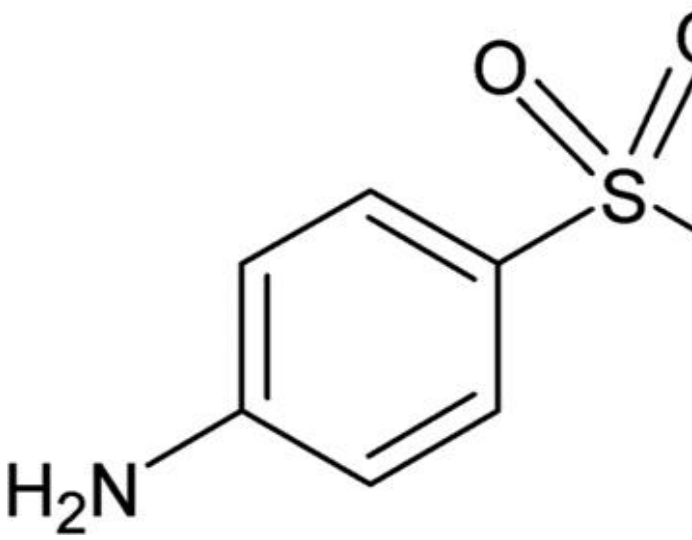
alt-text: Table 3

Table 3

iThe table layout displayed in this section is not how it will appear in the final version. The representation below is solely purposed for providing corrections to the table. To preview the actual presentation of the table, please view the Proof.

Main degradation products of sulfathiazole formed after coupling nZVI and Fenton processes, identified by HPLC-MS/MS, using the LightS

Degradation Products	Molecular formulas	m/z [M−H]$^+$	Proposed structures

4	C₃H₄N₂S	101	
5	C₆H₇NO₃S	174 → 132	
6	C₉H₉N₃S	192	

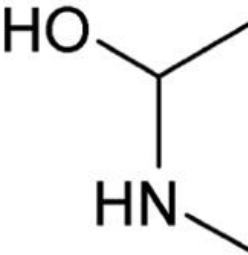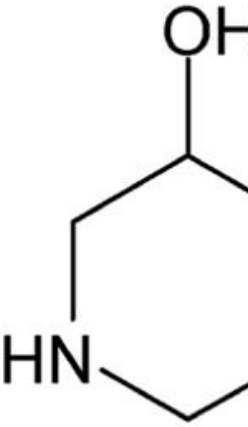| 7 | $C_9H_8N_2O_3S_2$ | $257 \rightarrow 174 \rightarrow 144 \rightarrow 118$ | |
| 8 | $C_9H_9N_3O_3S_2$ | $272 \rightarrow 208\,272 \rightarrow 172\,272 \rightarrow 101$ | |

Eight DPs were successfully detected in the degradation of NOR (Table 4). The single attack of the piperazine ring by •OH generated three DPs with m/z 334, 348 [23,52], and 336 [53]. Afterwards, DP with m/z 348 would break to form DP with m/z 294 [23,54]. When two •OH radicals attacked the piperazine ring, isomers with m/z 350 could be formed [55]. DP with m/z 251 was also found by Ahmad et al. [54], who studied the UV-photodegradation of NOR in aqueous solution (pH range 2–12), and by Chen and Chu [52], in the photocatalytic degradation of NOR over bismuth tungstate. The fragmentation mechanisms are given in the Supplementary Material.
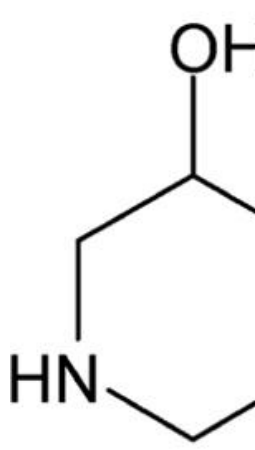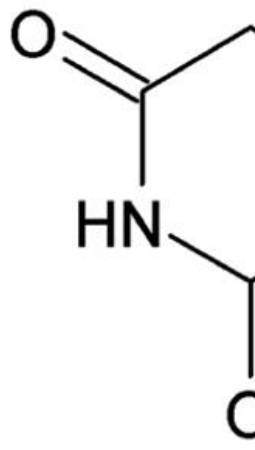
alt-text: Table 4
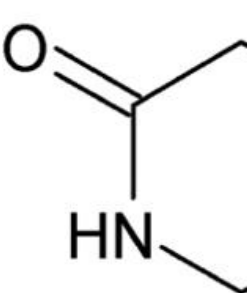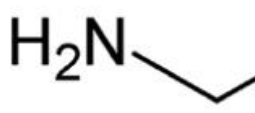
Table 4
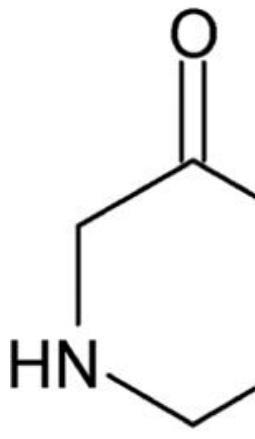
iThe table layout displayed in this section is not how it will appear in the final version. The representation below is solely purposed for providing corrections to the table. To preview the actual presentation of the table, please view the Proof.

Main degradation products of norfloxacin formed after coupling nZVI and Fenton processes, identified by HPLC-MS/MS, using the LightSi

Degradation Products	Molecular formulas	m/z [M−H]+	Proposed structures
9	$C_{16}H_{16}FN_3O_5$	$350 \rightarrow 332 \rightarrow 304 \rightarrow 275350 \rightarrow 332 \rightarrow 304 \rightarrow 249 \rightarrow 221$	
10	$C_{16}H_{16}FN_3O_5$	$350 \rightarrow 332 \rightarrow 304 \rightarrow 284350 \rightarrow 332 \rightarrow 304 \rightarrow 249$	

11	$C_{16}H_{18}FN_3O_4$	336 → 318 → 274336 → 294 → 249 → 221336 → 294 → 249 → 205 → 179	
12	$C_{16}H_{16}FN_3O_5$	350 → 332 → 304 → 278350 → 332 → 304 → 234	

13	$C_{12}H_{11}FN_2O_3$	$251 \rightarrow 233 \rightarrow 205 \rightarrow 153$	
14	$C_{16}H_{14}FN_3O_5$	$348 \rightarrow 330 \rightarrow 274 \rightarrow 231$	

| 15 | $C_{14}H_{17}FN_3O_3$ | $294 \rightarrow 276 \rightarrow 259 \rightarrow 231294 \rightarrow 224 \rightarrow 196 \rightarrow 167294 \rightarrow 250 \rightarrow 230$ | |
| 16 | $C_{16}H_{16}FN_3O_4$ | $334 \rightarrow 278 \rightarrow 208334 \rightarrow 278 \rightarrow 234 \rightarrow 214$ | |

3.3

Ecotoxicity ~~Estimation~~estimation

Based on the structures of SMT, STZ, NOR, and the proposed DPs, their corresponding ecotoxicological endpoints were estimated (Fig. 5). It is noteworthy that SMT and STZ are approximately two (acute) and three (chronic) orders of magnitude more ecotoxic than NOR.

alt-text: Fig. 5

Fig. 5

- 0
-
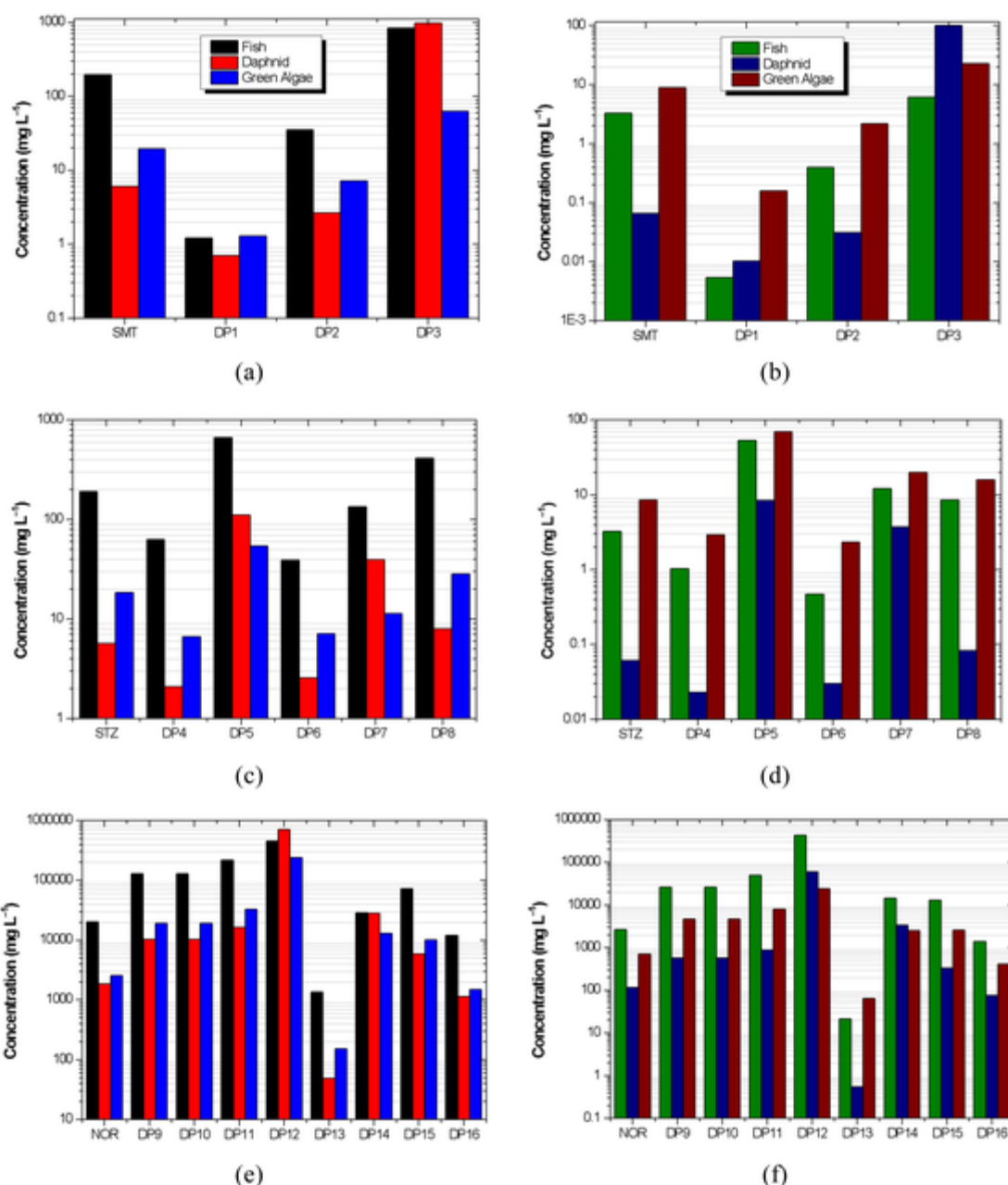
. (a, c, and e) Acute and (b, d, and f) chronic ecotoxicities estimates using ECOSAR 2.0. One can observe that, in general, when SMT and STZ were treated by the proposed coupling (nZVI + Fenton), more ecotoxic substances were generated. Of the eight detected DPs, five are more ecotoxic than the parent compounds. On the contrary, only two among the eight detected DPs are more ecotoxic than NOR. In fact, DP9, DP10, DP12, DP14, and DP16 are considered to be non-toxic substances. As their estimated endpoints exceed the water solubility by ten times or more, no effects at saturation (NES) are typically reported [40]. Another finding was that all of the DPs which presented increased ecotoxicity (DP1, DP2, DP4, DP6, DP8, and DP13) had one feature in common: they were all aromatic amines. Many aromatic amines have been reported to be powerful carcinogens, mutagens, and/or hepatotoxicants [56]. The chemical reactivity of the amino group depends on the mesomeric interaction with the aromatic system, which is determined by further substituents and steric factors. Both acute and chronic toxicities depend on the metabolic activation of the amino group. The key reaction responsible for the biological activity is the *N*-oxidation to aryl-*N*-hydroxylamines [57].

3.4

Biological ~~Tests~~tests

Neither the initial solutions nor the treated ones were toxic towards *Lactuca sativa*. As the initial concentrations of SMT, STZ, and NOR were all 1.0 mg L^{-1}, their respective DPs were in the µg L^{-1} to ng L^{-1} range. Therefore, although DPs with increased ecotoxicity might have been generated during degradation, their concentrations would be lower than the ecotoxicological endpoints (LC$_{50}$ and EC$_{50}$). That would explain why no ecotoxicity towards *L. sativa* could be observed.

Regarding the antibacterial activity removal, using *Escherichia coli* as the target organism, the initial antibiotics solutions significantly inhibited the growth of *E. coli* colonies, as expected, and after the nZVI treatment, that inhibition was significantly reduced. One can assign that reduction to the antibiotics degradation and/or to the generation of DPs with reduced or no antibacterial activity.

After the sequential Fenton process, the antibacterial activity of the antibiotics (and related DPs) was further removed. But that removal was not statistically significant for SMT and STZ (Fig. 6).

alt-text: Fig. 6

Fig. 6

- 0
-
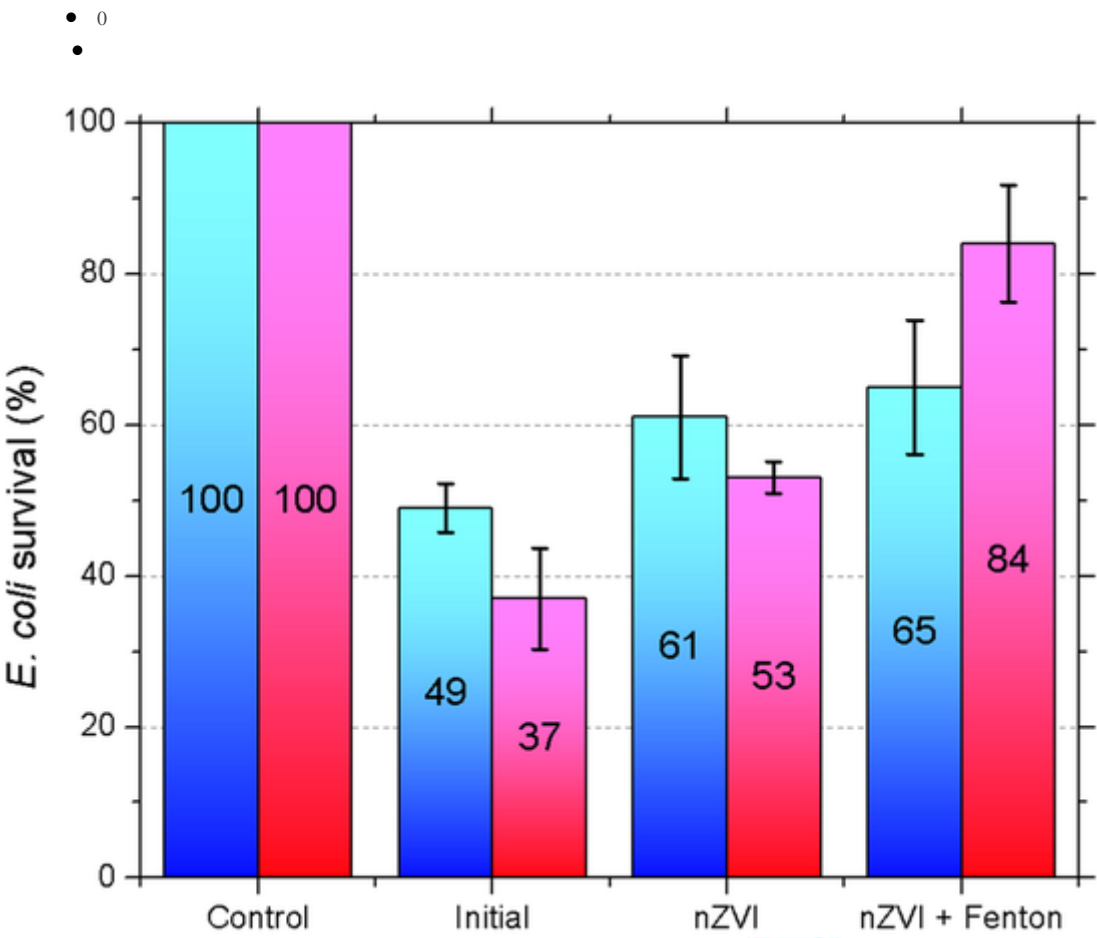
Survival indexes (averaged) of *Escherichia coli* cultures, (red) sulfamethazine and sulfathiazole; (blue) norfloxacin.

4

~~CONCLUSIONS~~Conclusions

Fe⁰ nanoparticles (size < ~~100~~100 nm, in average) were successfully and easily synthesized. Their spherical morphology and the presence of Fe⁰ and hydrated iron oxides were verified. The zero-valent iron process alone was not efficient for degrading ~~1.0~~1.0 mg L⁻¹ aqueous sulfamethazine, sulfathiazole, or norfloxacin. However, when the dissolved Fe(II) residue was used as the Fenton reagent (together with hydrogen peroxide), the antibiotics concentrations were below the method detection limit, meaning more than 96% degradation. Many degradation products could be identified, mainly generated by the attack of hydroxyl radicals to the antibiotics, as expected.

It is important to highlight that those results were achieved in a single pass through the system (no recycle) and that steady-state conditions were established after ~~15~~15 min. Moreover, due to the small Fe(II) concentrations after the zero-valent process (and before the Fenton one), reduced sludge formation was observed and "discharge" dissolved Fe(II) concentrations were kept low (< ~~1~~1 mg L⁻¹).

Regarding the biological activity of the generated effluent, no ecotoxicity towards *Lactuca sativa* was generated during degradation. Although degradation products with increased ecotoxicity might have been formed, their concentrations were lower than the respective ecotoxicological endpoints. However, the antimicrobial activity (*Escherichia coli*) could not be completely removed, mainly when sulfamethazine and sulfathiazole are considered. Therefore, further improvements should be made to the system in order to render the effluent safe to be discarded, without posing any risks of developing bacterial resistance.

In summary, the results pointed out that coupling the zero-valent iron process to the Fenton one is a promising approach for the treatment of antibiotics-laden waters, due to its ease of operation, reasonably high degradation performance, and reduced treatment time.

Uncited reference

[58].

CRediT authorship contribution statement

Ana Luiza Fornazaria: Conceptualization, Methodology, Formal analysis, Investigation, Data curation, Writing - original draft, Writing - review & editing, Visualization. **Vanessa Feltrin Labriola:** Data curation, Writing – review & editing, Visualization. **Bianca Ferreira da Silva:** Methodology, Formal analysis. **Lucas Fernandes Castro:** Methodology, Formal analysis. **Janice Rodrigues Perussi:** Resources, Writing – review & editing. **Eny Maria Vieira:** Resources, Writing – review & editing. **Eduardo Bessa Azevedo:** Conceptualization, Resources, Data curation, Writing – review & editing, Supervision.

Declaration of Competing Interest

The authors declare that they have no known competing financial interests or personal relationships that could have appeared to influence the work reported in this paper.

Appendix A

Supporting information

Supplementary data associated with this article can be found in the online version at doi:10.1016/j.jece.2021.105761.

~~REFERENCES~~References

- [1]Patel M., Kumar R., Kishor K., Mlsna T., Pittman Junior C.U., Mohan D., Pharmaceuticals of emerging concern in aquatic systems: chemistry, occurrence, effects and removal methods, ~~Chemical Reviews~~Chem. Rev. 119 (2019) 3510–3673, doi:10.1021/acs.chemrev.8b00299.

- [2]Khan N.A., Khan S.U., Ahmed S., Farooqi I.H., Yousefi M., Mohammadi A.A., Changani F., ~~Recent trends in disposal and treatment technologies of emerging-pollutants- A critical review~~Recent trends in disposal and treatment technologies of emerging-pollutants- a critical review, ~~TrAC Trends in Analytical Chemistry~~TrAC Trends Anal. Chem. 122 (2020) 115744, doi:10.1016/j.trac.2019.115744.

- [3]Batista A.P.S., Nogueira R.F.P., Parameters affecting sulfonamide photo Fenton degradation – iron complexation and substituent group, ~~Journal of Photochemistry and Photobiology A: Chemistry~~J. Photochem. Photobiol. A Chem. 232 (2012) 8–13, doi:10.1016/j.jphotochem.2012.01.016.

- [4]Khan A.H., Aziz H.A., Khan N.A., Hasan M.A., Ahmed S., Farooqi I.H., Dhingra A., Vambol V., Changani F., Yousefi M., Islam S., Mozaffari N., Mahtab M.S., ~~Impact, disease outbreak and the eco-hazards associated with pharmaceutical residues: A critical review~~Impact, disease outbreak and the eco-hazards associated with pharmaceutical residues: a critical review, ~~International Journal of Environmental Science and Technology~~Int. J. Environ. Sci. Technol. (2021), doi:10.1007/s13762-021-03158-9.

- [5]Das N., Madhavan J., Selvi A., Das D., An overview of cephalosporin antibiotics as emerging contaminants: a serious environmental concern, 3 Biotech 9 (6) (2019) 1–14, doi:10.1007/s13205-019-1766-9.

- [6]Rajeev L., ~~Antibiotic Discovery~~Antibiotic discovery, ~~Mater Methods~~Mater. Methods 8 (2671) (2020), doi:10.13070/mm.en.8.2671.

- [7]Fair R.J., Tor Y., Antibiotics and bacterial resistance in the 21st century, ~~Perpectives in Medicinal Chemistry~~Perpectives Med. Chem. 6 (2014) 25–64, doi:10.4137/pmc.s14459.

- [8]~~Greenwood, D. Chapter 29 - Sulfonamides. Saunders. In: Antibiotic and Chemotherapy (Ninth ed.), London, 337-343, 2010.~~Greenwood, D. Chapter 29 - Sulfonamides. Saunders. In: Antibiotic and Chemotherapy (Ninth ed.), London, 337–343, 2010. https://doi.org/10.1016/b978–0-7020–4064-1.00029–4.

- [9]King D.E., Malone R., Lilley S.H., New classification and update on the quinolone antibiotics, ~~American Family Physician~~Am. Fam. Physician 61 (9) (2000) 2741–2748. https://pubmed.ncbi.nlm.nih.gov/10821154/.

- [10]Rasheed T., Bilal M., Nabeel F., Adeel M., Iqbal H.M.N., Environmentally-related contaminants of high concern: potential sources and analytical modalities for detection, quantification, and treatment, Environment International Environ. Int. 122 (2019) 52–66, doi:10.1016/j.envint.2018.11.038.

- [11]Feng J.L., Liu Q., Ru X.L., Xi N.N., Sun J.H., Occurrence and distribution of priority pharmaceuticals in the Yellow River and the Huai in Henan, China, Environmental Science and Pollution Research Environ. Sci. Pollut. Res. 27 (14) (2020) 16816–16826, doi:10.1007/s11356-020-08131-6.

- [12]Zang Y.Y., Rong C., Song Y.Q., Wang Y.H., Pei J.Y., Tang X.Y., Zang R.J., Yu K.F., Oxidation of antibacterial agent norfloxacin during sodium hypochlorite disinfection of marine culture water, Chemosphere 182 (2017) 245–254, doi:10.1016/j.chemosphere.2017.05.023.

- [13]Liu H.G., Zhou X.Y., Huang H.X., Zhang J.S., Prevalence of antibiotic resistance genes and their association with antibiotics in wastewater treatment plant: Process distribution and analysis Prevalence of antibiotic resistance genes and their association with antibiotics in wastewater treatment plant: process distribution and analysis, Water 11 (2495) (2019) 1–14, doi:10.3390/w11122495.

- [14]Rodriguez-Mozaz S., Chamorro S., Marti E., Huerta B., Gros M., Sànchez-Melsió A., Borrego C.M., Barceló D., Balcázar J.L., Occurrence of antibiotic resistance genes in hospital and urban wastewaters and their impact on the receiving river, Water Research Water Res. 69 (1) (2015) 234–242, doi:10.1016/j.watres.2014.11.021.

- [15]Ngigi A.N., Magu M.M., Muendo B.M., Occurrence of antibiotics residues in hospital wastewater treatment plant, and in surface water in Nairobi Conty, Kenya, Environmental Monitoring and Assessment Environ. Monit. Assess. 192 (18) (2020) 1–16, doi:10.1007/s10661-019-7952-8.

- [16]Fu F., Dionysiou D.D., Liu H., The use of zero-valent iron for groundwater remediation and wastewater treatment: a review, Journal of Hazardous Materials J. Hazard. Mater. 267 (2014) 194–205, doi:10.1016/j.jhazmat.2013.12.062.

- [17]Filip J., Karlincky F., Marusak Z., Lazar P., Cernik M., Otyepka M., Zboril R., Anaerobic reaction of nanoscale zerovalent iron with water: mechanism and kinetics 13817-1385 The Journal of Physical Chemistry C J. Phys. Chem. C 118 (25) (2014) 13817–13825, doi:10.1021/jp501846f.

- [18]Li X., Elliot D.W., Zhang W., Zero-valent iron nanoparticles for abatement of environmental pollutants: materials and engineering aspects, Critical Reviews in Solid State and Materials Sciences Crit. Rev. Solid State Mater. Sci. 31 (4) (2006) 111–122, doi:10.1080/10408430601057611.

- [19]Goswami A., Jiang J., Comparative performance of catalytic Fenton oxidation with Zero-Valent iron (Fe0) in comparison with ferrous sulphate for removal of micropollutants, Applied Sciences Appl. Sci. 9 (11) (2019) 1–15, doi:10.3390/app9112181.

- [20]Feng W., Nansheng D., Photochemistry of hydrolytic iron (III) species and photoinduced degradation of organic compounds. A minireview, Chemosphere 41 (8) (2000) 1137–1147, doi:10.1016/s0045-6535(00)00024-2.

- [21]Babu D.S., Srivastava V., Nidheesh P., Kumar M.S., Detoxification of water and wastewater by advanced oxidation processes, ~~Science of The Total Environment~~Sci. Total Environ. 696 (2019) 133961, doi:10.1016/j.scitotenv.2019.133961.

- [22]~~Sweeny, K. H., Fischer, J. R. (1972). Reductive degradation of halogenated pesticides. US 3640821.~~Sweeny, K.H., Fischer, J.R. ,1972. Reductive degradation of halogenated pesticides. US 3640821.

- [23]Zhou T., Zou X., Mao J., Wang J., Synergistic degradation of antibiotic norfloxacin in a novel heterogeneous sonochemical Fe0/tetraphosphate Fenton-like system, ~~Ultrasonics Sonochemistry~~Ultrason. Sonochem. 37 (2017) 320–327, doi:10.1016/j.ultsonch.2017.01.015.

- [24]Ghauch A., Tuqan A., Assi H.A., Antibiotic removal from water: elimination of amoxicillin and ampicillin by microscale and nanoscale iron particles, ~~Environmental Pollution~~Environ. Pollut. 157 (5) (2009) 1626–1635, doi:10.1016/j.envpol.2008.12.024.

- [25]Fang Z., Chen J., Qiu X., Cheng W., Zhu L., Effective removal of antibiotic metronidazole from water by nanoscale zero-valent iron particles, Desalination 268 (~~1–3~~1–3) (2011) 60–67, doi:10.1016/j.envpol.2008.12.024.

- [26]Perine J.A.L., Silva B.F., Nogueira R.F.P., Zero-valent iron mediated degradation of ciprofloxacin – assessment of adsorption, operation parameters and degradation products, Chemosphere 117 (2014) 345–352, doi:10.1016/j.chemosphere.2014.07.071.

- [27]Daneshkhah M., Hossaini H., Malakootian M., Removal of metoprolol from water by sepiolite-supported nanoscale zero-valent iron, ~~Journal of Environmental Chemical Engineering~~J. Environ. Chem. Eng. 5 (4) (2017) 3490–3499, doi:10.1016/j.jece.2017.06.040.

- [28]San Román I., Galdames A., Alonso M.L., Bartolomé L., Vilas J.L., Alonso R.M., Effect of coating on the environmental applications of zero valent iron nanoparticles: the lindane case, ~~Science of the Total Environment~~Sci. Total Environ. 565 (2016) 795–803, doi:10.1016/j.scitotenv.2016.04.034.

- [29]Bagbi Y., Sarswat A., Tiwari S., Mohan D., Pandey D., Solanki P.R., Nanoscale zero-valent iron for aqueous lead removal, ~~Advanced Materials Proceedings~~Adv. Mater. Proc. 2 (4) (2017) 235–241, doi:10.5185/amp.2017/407.

- [30]Adio S.O., Omar M.H., Asif M., Saleh T.A., ~~Arsenic and selenium removal from water using biosynthesized nanoscale zero-valent iron: A factorial design analysis~~Arsenic and selenium removal from water using biosynthesized nanoscale

- zero-valent iron: a factorial design analysis, Process Saf. Environ. Prot. 107 (2017) 518–527, doi:10.1016/j.psep.2017.03.004.

- [31]Xie Y., Yi Y., Qin Y., Wang L., Liu G., Wu Y., Diao Z., Zhou T., Xu M., Perchlorate degradation in aqueous solution using chitosan-stabilized zero-valent iron nanoparticles, Sep. Purif. Technol. 171 (2016) 164–173, doi:10.1016/j.seppur.2016.07.023.

- [32]Gonçalves J.R., The soil and groundwater remediation with zero valent iron nanoparticles, Procedia Eng. 143 (2016) 1268–1275, doi:10.1016/j.proeng.2016.06.122.

- [33]Ponder S.M., Darab J.G., Mallouk T.E., Remediation of Cr(VI) and Pb(II) aqueous solutions using supported, nanoscale zero-valent iron, Environ. Sci. Technol. 34 (12) (2000) 2564–2569, doi:10.1021/es9911420.

- [34]Donadelli J.A., Berardozzi E., Carlos L., Einschlag F.S.G., Continuous treatment of an azo dye based on a combined ZVI/photo-Fenton setup. Process modelling by response surface methodology, J. Water Process Eng. 37 (101480) (2020), doi:10.1016/j.jwpe.2020.101480.

- [35]Zhang W., Cheng Y., Gao Y., Chen Z., Megharaj M., Naidu R., Rapid and complete dechlorination of PCP in aqueous solution using Ni-Fe nanoparticles under assistance of ultrasound, Chemosphere 65 (1) (2006) 58–94, doi:10.1016/j.chemosphere.2006.02.060.

- [36]APHA/AWWA/WEF, Standard Methods for the Examination of Water and Wastewater, twenty-first ed., Amer Public Association, Washington DC, 2005.
- [37]Nogueira R.F.P., Oliveira M.C., Paterlini W.C., Simple and fast spectrophotometric determination of H_2O_2 in photo-Fenton reactions using metavanadate, Talanta 66 (2005) 86–91, doi:10.1016/j.talanta.2004.10.001.

- [38]Bairán G., Rebollar-Pérez G., Chávez-Bravo E., Torres E., Treatment processes for microbial resistance mitigation: the technological contribution to tackle the problem of antibiotic resistance, Int. J. Environ. Res. Public Health 17 (23) (2020) 8866, doi:10.3390/ijerph17238866.

- [39]Barancheshme F., Munir M., Development of antibiotic resistance in wastewater treatment plants, in: Kumar Y. (Ed.), Antimicrobial Resistance - A Global Threat, IntechOpen Limited, London, 2019, pp. 75–92.

- [40]United States Environmental Protection Agency (USEPA). https://www. epa.gov/tsca-screening-tools/ecological-structure-activity-relationships-ecosar-predictive-model, 2021 (Accessed 31 February 2021).

- [41]Rossi D., Beltrami M., Sediment ecological risk assessment: in situ and laboratory toxicity testing of Lake Orta sediments, Chemosphere 37 (~~14-15~~14–15) (1998) 2885–2894, doi:10.1016/S0045-6535(98)00330-0.

- [42]Ortega M.C., Moreno M.T., Ordovas J., Aguado M.T., Behavior of different horticultural species in phytotoxicity bioassays of bark substrates, ~~Scientia Horticulturae~~Sci. Hortic. 66 (~~1-2~~1–2) (1996) 125–132, doi:10.1016/0304-4238(96)00900-4.

- [43]Stevens M.G., Olsen S.C., Comparative analysis of using MTT and XTT in colorimetric assays for quantitating bovine neutrophil bactericidal activity, ~~Journal of Immunological Methods~~J. Immunol. Methods 157 (~~1-2~~1–2) (1993) 225–231, doi:10.1016/0022-1759(93)90091-k.

- [44]Papapanagiotou E.P., Fletouris D.J., Psomas E.I., Effect of various heat treatments and cold storage on sulfamethazine residues stability in incurred piglet muscle and cow milk samples, ~~Analytica Chimica Acta~~Anal. Chim. Acta 529 (2005) 305–309, doi:10.1016/j.aca.2004.09.029.

- [45]Noa M., Perez N., Gutierrez R., Escobar I., Diaz G., Stability of sulfonamides nitrofurans and chloramphenicol residues in preserved raw milk samples measured by liquid chromatography, ~~Journal of AOAC International~~J. AOAC Int. 85 (6) (2002) 1415–1419, doi:10.1093/jaoac/85.6.1415.

- [46]García-Galán M.J., Días-Cruz M.S., Barceló D., Kinetic studies and characterization of photolytic products of sulfamethazine, sulfapyridine and their acetylated metabolites in water under simulated solar irradiation, ~~Water Research~~Water Res. 46 (2012) 711–722, doi:10.1016/j.watres.2011.11.035.

- [47]Gao J., Hedman C., Liu C., Guo T., Pedersen J.A., Transformation of sulfamethazine by manganese oxide in aqueous solution, ~~Environmental Science & Technology~~Environ. Sci. Technol. 46 (2012) 2642–2651, doi:10.1021/es202492h.

- [48]Ji Y., Shi Y., Wang L., Lu J., Ferronato C., Chovelon J., Sulfate radical-based oxidation of antibiotics sulfamethazine, sulfapyridine, sulfadiazine, sulfadimethoxine, and sulfachloropyridazine: formation of SO_2 extrusion products and effects of natural organic matter, ~~Science of the Total Environment~~Sci. Total Environ. ~~593-594~~593–594 (2017) 704–712, doi:10.1016/j.scitotenv.2017.03.192.

- [49]Yi Z., Wang J., Jiang T., Tang Q., Cheng Y., Photocatalytic degradation of sulfamethazine in aqueous solution using ZnO with different morphologies, ~~Royal Society Open Science~~R. Soc. Open Sci. 5 (4) (2018) 1–11, doi:10.1098/rsos.171457.

- [50]Feng Y., Liu J., Wu D., Zhou Z., Deng Y., Zhang T., Kaimin S., Efficient degradation of sulfamethazine with CuCo2O4 spinel nanocatalysts for peroxymonosulfate activation, ~~Chemical Engineering Journal~~Chem. Eng. J. 280 (2015) 514–524, doi:10.1016/j.cej.2015.05.121.

- [51]Oh W., Chang V.W.C., Hu Z., Goei R., Lim T., Enhancing the catalytic activity of g-C3N4 through Me doping (Me = Cu, Co and Fe) for selective sulfathiazole

degradation via redox-based advanced oxidation process, ~~Chemical Engineering Journal~~Chem. Eng. J. 323 (2017) 260–269, doi:10.1016/j.cej.2017.04.107.

- [52]Chen M., Chu W., Photocatalytic degradation and decomposition mechanism of fluoroquinolones norfloxacin over bismuth tungstate: experiment and mathematic model, ~~Applied Catalysis B: Environmental~~Appl. Catal. B Environ. ~~168-169~~168–169 (2015) 175–182, doi:10.1016/j.apcatb.2014.12.023.

- [53]Prieto A., Möder M., Rodil R., Adrian L., Urea-Marco E., Degradation of the antibiotics norfloxacin and ciprofloxacin by a white-rot fungus and identification of degradation products, ~~Bioresurces Tecnhology~~Bioresur. Tecnhol. 102 (2011) 10987–10995, doi:10.1016/j.biortech.2011.08.055.

- [54]Ahmad I., Bano R., Musharraf S.G., Sheraz M.A., Ahmed S., Tahir H., Ul Arfeen Q., Bhatti M.S., Shad Z., Hussain S.F., Photodegradation of norfloxacin in aqueous and organic solvents: A kinetic study, ~~Journal of Photochemistry and Photobiology A: Chemistry~~J. Photochem. Photobiol. A Chem. 302 (2015) 1–10, doi:10.1016/j.jphotochem.2015.01.005.

- [55]Ding D., Liu C., Ji Y., Yang Q., Chen L., Jiang C., Cai T., Mechanism insight of degradation of norfloxacin by magnetite nanoparticles activated persulfate: Identification of radicals and degradation pathway, ~~Chemical Engineering Journal~~Chem. Eng. J. 308 (2017) 330–339, doi:10.1016/j.cej.2016.09.077.

- [56]Benigni R., Passerini L., Carcinogenicity of the aromatic amines: from structure–activity relationships to mechanisms of action and risk assessment, ~~Mutation Research/Reviews in Mutation Research~~Mutat. Res. /Rev. Mutat. Res. 511 (3) (2002) 191–206, doi:10.1016/s1383-5742(02)00008-x.

- [57]International Agency for Research on Cancer (IARC), Some Aromatic Amines, Organic Dyes, and Related Exposures, Lyon (FR), International Agency for Research on Cancer, 2010. https://www.ncbi.nlm.nih.gov/books/NBK385423/.

- ~~[58]Dickinson M., Scott T.B., The application of zero-valent iron nanoparticles for the remediation of a uranium contaminated waste effluent, Journal of Hazardous Materials 178 (1-3) (2010) 171–179, doi:10.1016/j.jhazmat.2010.01.060~~